A new methodological approach: The combined use of two-stage streaker samplers and optical particle counters for the

Available online at www.sciencedirect.com
ScienceDirect
Atmospheric Environment 41 (2007) 5525–5535
ATMOSPHERIC ENVIRONMENT
www.elsevier.com/locate/atmosenv

Technical note

A new methodological approach: The combined use of two-stage streaker samplers and optical particle counters for the characterization of airborne particulate matter

Federico Mazzei[a], Franco Lucarelli[b], Silvia Nava[b], Paolo Prati[a,*], Gianluigi Valli[c], Roberta Vecchi[c]

[a]*Dipartimento di Fisica and INFN, via Dodecaneso 33, 16146 Genova, Italy*
[b]*Dipartimento di Fisica and INFN, via Sansone 1, 50019 Sesto Fiorentino, Italy*
[c]*Istituto di Fisica Generale Applicata and INFN, via Celoria 16, 20133 Milano, Italy*

Received 17 January 2007; received in revised form 2 April 2007; accepted 11 April 2007

Abstract

We describe a new experimental methodology based on the contemporary use of two-stage continuous streaker samplers and optical particle counters. This is a complementary approach to size-segregated particulate matter (PM) sampling, and it is able to give information on the elemental size distribution and to assess the contribution of major PM source to size bins. PM samples in the fine and coarse fraction of PM10 have been collected by a two-stage streaker sampler and analyzed by particle-induced X-ray emission (PIXE) to obtain elemental concentration time series with hourly resolution. PM sources and profiles were singled out by positive matrix factorization (PMF). A multi-linear regression of size-segregated number of particles versus the sources, resolved by PMF, made possible the apportionment of size-segregated particles number in a fast and direct way. Results obtained in three sampling sites, located in different urban districts are discussed.

Keywords: Particulate matter; Streaker sampler; Optical counter; PIXE; PMF

1. Introduction

1.1. Particulate matter characterization

Particulate matter (PM) is an important factor in producing environmental impact as well as adverse human health effects. Many epidemiological studies have shown a correlation between the increase of PM concentration and morbidity and/or mortality (HEI, 2002; Pope et al., 2002; Balásházy et al., 2003 and references therein). PM is routinely monitored in several countries, according to present legislation, in terms of daily average concentration in the PM10 and PM2.5 fractions (i.e. concentration of particles in atmosphere with aerodynamic diameter smaller than 10 and 2.5 μm, respectively). In some cases, samples collected for regulatory purposes are also analyzed to determine their composition. The compositional information is useful not only to assess the concentration of peculiar (and in same

*Corresponding author. Tel.: +39 10 3536439; fax: +39 10 314218.
E-mail address: prati@ge.infn.it (P. Prati).

1352-2310/$ - see front matter © 2007 Elsevier Ltd. All rights reserved.
doi:10.1016/j.atmosenv.2007.04.012

cases toxic) elements but also to identify PM sources, their emission profile and loading. The receptor models approach (Gordon, 1988) is often exploited with this aim. Actually, a complete characterization of atmospheric PM would require several other information, such as the temporal behaviour of PM and its compounds on a short-time basis (i.e. from minutes to hours, especially in urban and/or industrial areas), the size-segregated distribution of PM and its components as well as the particles number distribution with high-time resolution. All these additional features help both in the source characterization and in the assessment of health effects. In particular, since a correlation between morbidity and particles number, namely for particles with diameter smaller than 1 μm, has been claimed in some studies (Wichmann and Peters, 2000 and references therein), it would be of interest to single out the relationship among specific size ranges and PM sources.

1.2. Instruments

A large number of instruments have been developed in the last years and they are widely used to accomplish the tasks quoted above. Nevertheless, while several devices have been manufactured and are commercially available to count particles and to measure their size distribution with high-time resolution (Knutson and Whitby, 1975; Büttner, 1990; Fissan et al., 1984; Winklmayr et al., 1991 and others), the assessment of elements and/or compounds size distribution is still quite tricky. Size-segregated elemental concentration is commonly measured by cascade impactors (Hillamo and Kauppinen, 1991; Marple et al., 1991; Maenhaut et al., 1996) but very hardly they can be used to obtain long temporal trends since any set of filters should be kept under sampling for a few hours and then manually substituted. As a matter of fact, sampling campaigns using impactors often last a few days with a quite limited number of samples collected (Salma et al., 2005 and references therein). A research group at Davis University, CA, developed the DRUM multi-stage continuous impactor (Cahill et al., 1987) which separates PM in eight (more frequently three) size intervals on suitable filter tapes, producing a continuous PM deposition for 6 weeks with a 3 h time resolution. The PM deposits obtained by this very powerful device can be suitably analyzed with synchrotron radiation X-ray fluorescence (SR-XRF) (Bukowiecki et al., 2005 and references therein) in short irradiation times (about 30 s for each 3 h with a minimum detection limit (MDL) of 0.1 ng m^{-3}); unfortunately, SR-XRF facilities are not always easily accessible. Using a more standard ion beam analysis (IBA) technique, the time required to analyze a DRUM set of samples would be significantly higher. Another possibility to perform size-segregated PM samplings with high time resolution are two-stage streaker samplers (Annegarn et al., 1988), which collect the fine and coarse fraction of PM10: typically, on each couple of collecting frames the sampling lasts 1/2 weeks and elemental concentrations with hourly/2-hourly time resolution can be obtained. Particle-induced X-ray and gamma emission (PIXE and PIGE) are frequently exploited to analyze streaker frames: at the new Laboratorio di tecniche nucleari per i Beni Culturali (LABEC), Istituto Nazionale di Fisica Nucleare (I.N.F.N.) accelerator facility in Florence (Calzolai et al., 2006) recent developments (Chiari et al., 2005) make possible the analysis of one streaker frame (168 spots) with 9 h of beam time.

We present here the results of the combined use of a streaker sampler and an optical particle counter (OPC).

OPCs are widespread real-time instruments based on the principle of light scattering from particles. They provide both the size and the number of particles in several size bins with short-time resolution (i.e. from seconds to hours) and thus their output can be compared with elemental concentration time series. A significant drawback with OPCs is that the conversion from optical sizes to aerodynamic diameters is not trivial (Binnig et al., 2007 and references therein). Our approach gives information on the size distribution of PM elements and on the PM sources contributing to different size ranges. Data analysis is relatively fast and thus, this methodology could be useful when long term and time-resolved elemental concentrations are available.

2. Material and methods

2.1. Sampling and on-site measurements

PM has been collected by two-stage streaker samplers (Pixe International Corporation, USA). The streaker consists of a pre-impactor that removes particles with aerodynamic diameter $D_{ae} > 10\,\mu m$ from the incoming air flux, a thin Kapton foil which collects particles with

$2.5\,\mu m < D_{ae} < 10\,\mu m$ and a Nuclepore film (pore size: 0.4 μm) that intercepts all smaller particles. The sampling produces a circular continuous deposit on the two stages. The deposits can be analyzed by IBA to obtain elemental concentrations with hourly resolution.

The particles number distribution was measured by a Grimm 1.108 OPC, in 32 size intervals with diameters in the 0.25–32 μm size range with a 30 min time resolution. In one site (Cornigliano), the OPC was operated with an older software version which classified particles in 15 size channels (in the 0.35–32 μm size range). The Grimm OPC uses a patented dehumidification system which operates when ambient relative humidity is higher than 70%. This OPC has a patented light-scattering technique based on an advanced low water-sensitive laser source ($\lambda = 675$ nm). The OPC is factory calibrated via monodisperse Latex for size classification. The reproducibility of the OPC in particle counting is ±2% (Putaud et al., 2004).

It is noteworthy that the streaker sampler consists of two inertial impaction stages which select particles on the basis of their aerodynamic diameter (D_{ae}), while the OPC measures the particles optical diameter (D_p) at ambient conditions. The link between the two quantities depends on particle density and on refractive index which vary with particle composition so that distributions obtained by different methods can differ considerably (Hand and Kreidenweis, 2002). A detailed discussion on this issue is outside the scope of this work and in the following text we only refer to optical diameter measured by OPC.

Experiments were organized in several sites between March and December 2005. Sampling sites were all located in the urban area of Genoa (Italy), in nodes of the municipal air quality network: Cornigliano, Multedo and Lanterna. Cornigliano is an industrial site near a large steel plant, Multedo is located close to an heavy-traffic road in the town outskirts and the Lanterna site is in the harbour area. The three sites are aligned along the sea coast on a East–West direction with mutual distances of a few kilometers. Typical sampling time was 1–2 weeks per site.

2.2. Laboratory and data analysis

PIXE analysis was performed on streaker deposits, using the external beam PIXE facility of the new LABEC I.N.F.N. Tandem accelerator at the Physics Department of the Florence University (Calzolai et al., 2006). PIXE spectra were fitted for 25 elements (Na, Mg, Al, Si, P, S, Cl, K, Ca, Ti, V, Cr, Mn, Fe, Ni, Cu, Zn, As, Se, Br, Sr, Zr, Mo, Ba, Pb) using the GUPIX software package (Maxwell et al., 1995) and the elemental concentrations were obtained via a calibration curve from a set of thin standards (Micromatter Inc., USA). MDLs change for each element in the range from 1 to 10 ng m^{-3}. Total mass concentration cannot be measured on streaker frames.

As first step in data reduction, we calculated the Pearson's correlation coefficients between elemental concentration time series and temporal trends for each size bin measured by the OPC and averaged on 1 h time interval. Patterns (i.e.: distribution of the correlation coefficients versus size bins, see section results) with significant differences and/or similarities from site to site were obtained. To explain these features, we processed all the data looking for major PM sources and their profiles. We applied the Positive Matrix Factorization (PMF) receptor model to the time series of hourly elemental concentrations. PMF is a least-squares formulation of factor analysis developed by Paatero (Paatero and Tapper, 1994): it assumes that the ambient aerosol characterization at one or more sites can be explained by the product of a source matrix and contribution matrix. The two matrices are obtained by an iterative minimization algorithm. PMF also weighs individual data points by their analytical uncertainties and constraints factor loading and factor scores to not-negative values. The not-negative constraint minimizes the ambiguity caused by factor rotation and gives a physical sense to the results. An important advantage of PMF is the possibility to handle missing data and values below detection limits, by underweighing these data points. The concentration values and their associated errors were treated according to the methodology suggested by Polissar et al. (1998). To reduce the influence of extreme values on the PMF solution, the robust mode was used. The determination of the optimal solution was performed following Lee et al. (1999) and the PMF diagnostics described therein; it is worth noting that PMF is a descriptive model and there is no objective criterion to choose the best solution (Paatero et al., 2002). In this work, the final solutions were determined by trial and error, choosing the most stable ones with respect to different input options and those with most physically meaningful profiles.

3. Results

3.1. Particles number distributions and elemental composition

Particle size distributions, measured by the OPC in the three sites are shown in Fig. 1. Concerning PIXE results, we compared the fine and coarse fraction concentration time series of each element: we summed the fine and coarse concentration of elements with well-correlated ($R^2 > 0.8$) time series in the two fractions, otherwise we maintained them separated. For some elements, weak correlations were due to the fact that, in one fraction, the concentration was often below MDL: in this case we again summed together the two series. Actually, S only showed a different time behaviour in the two fractions and in the analysis we kept its fine and coarse concentrations

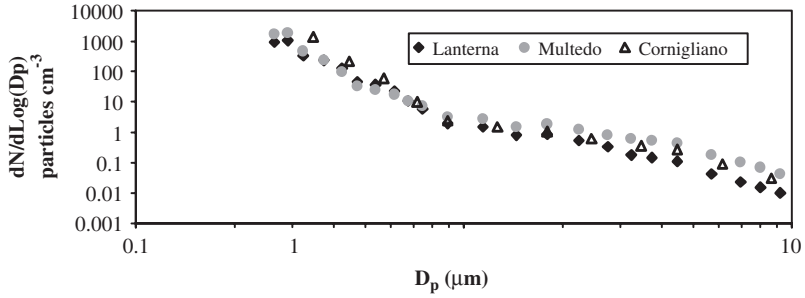

Fig. 1. Average particle size distributions. Measuring time was 1 week in Lanterna e Multedo and 2 weeks in Cornigliano.

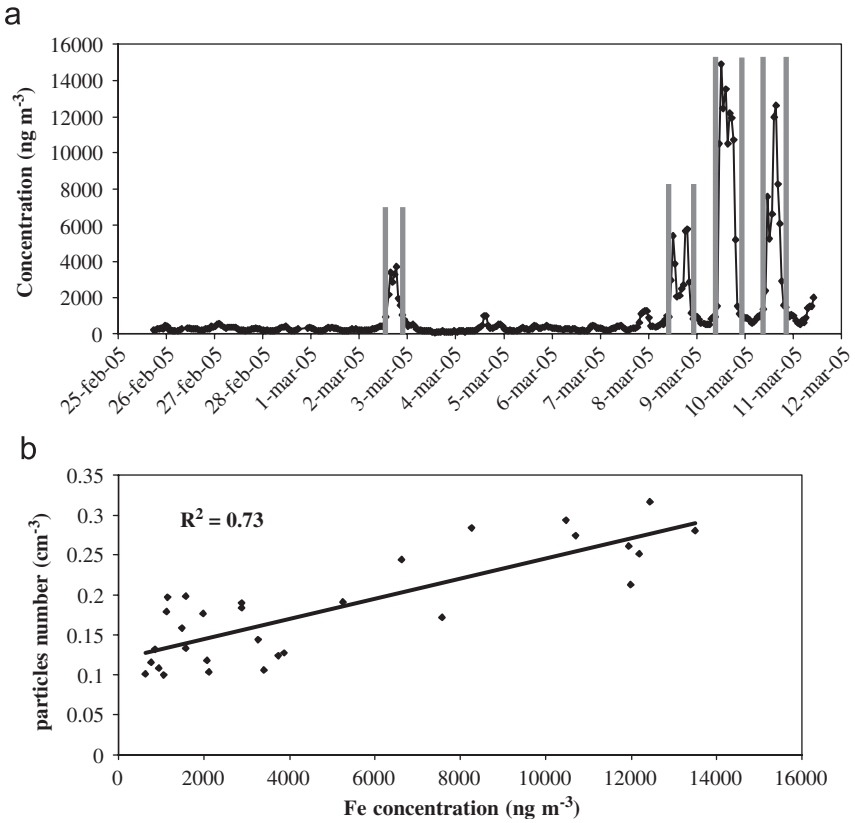

Fig. 2. (a) Time series of Fe concentration (fine + coarse) measured in Cornigliano, vertical gray lines delimit the time intervals selected to calculate the correlation coefficient between elemental data and size bins. (b) Fe concentration data and particles number in the size range $1.6\,\mu m < D_p < 2\,\mu m$ in the selected time intervals (30 points).

separated. Actually, previous works (Prati et al., 2000 and references therein) identified the sea as the dominant source of coarse S in Genoa. As a matter of fact, we used a reduced data set where all elemental concentrations in the fine and coarse fraction, except the case of sulphur, have been summed. Information on elemental size distributions can be obtained by the concentration time series given by streaker sampler, using the OPC data: we selected, for each element, time intervals corresponding to concentration peaks (Fe concentration temporal pattern is given as an example in Fig. 2(a) and we calculated the correlation coefficients between these selected data and the particles number in each size bin. During these episodes, the particles size distribution is likely to be more specific of the emitting source than during other sampling intervals because elemental concentration peaks have been typically observed in concomitance with the increase of source emissions, as detected also during previous work using high

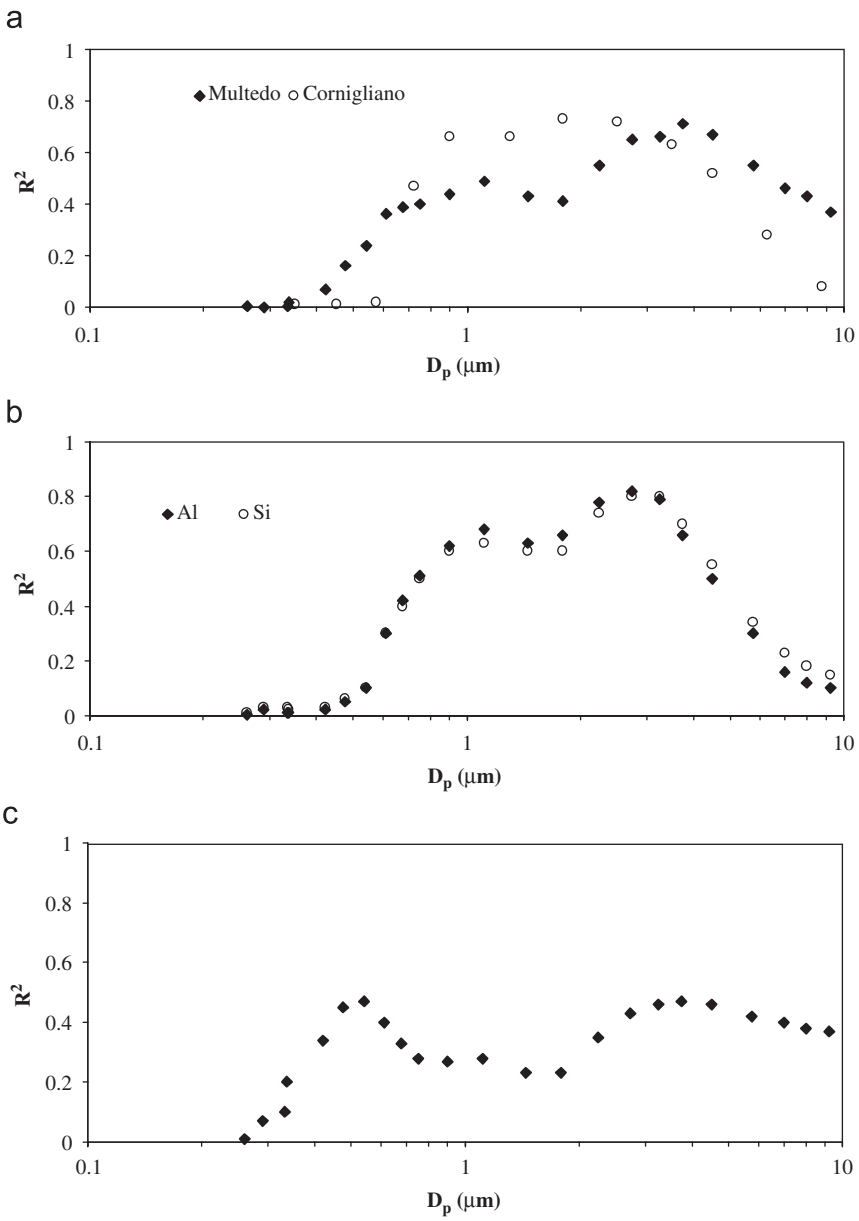

Fig. 3. Distribution of correlation coefficients between elemental concentration values and size bins. (a) Fe in Cornigliano and Multedo (30 and 60 points respectively); (b) Al and Si in Multedo (32 points); (c) Cu in Multedo (73 points).

time resolution (e.g. Prati et al., 2000 and references therein). In Fig. 2(b), the correlation coefficient between the selected Fe concentration values (Fig. 2(a)) and the number of particles with optical diameter between 1.6 and 2 μm are represented. In Figs. 3(a–c), some examples of correlation coefficients distributions versus the optical particle diameter are given; it should be noted that they cannot be interpreted as physical size distributions. Fe measured at the industrial site (Cornigliano) peaks around 2 μm (Fig. 3(a)): this is very likely related to emissions from a furnace blast which had been already found concentrated in the PM2.5 fraction by a PMF analysis on daily samples (Mazzei, 2007). In Multedo, we have a different behaviour with high correlation coefficients for larger particles, probably due to re-suspended soil dust, and similar patterns turn out for elements like Al and Si (Fig. 3(b)). Fe concentration measured at Lanterna is quite low and it does not show correlation with any size bin. In the site with the highest contribution from traffic (Multedo), Cu shows peaks around 0.5 and 3.5 μm (Fig. 3(c)), whereas in the other two sites, characterized by a lower impact of traffic emissions, the correlation coefficients are generally very low. Crustal elements have, as expected, higher correlation coefficients with size bins beyond 1 μm. On 18 July 2005, a long-range transport event from Sahara occurred: it was revealed by back trajectories, calculated by NOAA–HYSPLIT (Draxler and Rolph, 2003) and by simultaneous concentration peaks in soil-related elements. In Fig. 4 (data from

Table 1
Modes, in μm, of the correlation coefficients distribution between some elemental concentration and particles number time series

Elements	Cornigliano	Lanterna	Multedo
Si	1.0	1.9	1.1
	–	–	3.0
Cl	1.6	1.5	1.7
S_{fine}	0.45	0.37	0.28
Fe	2.0	–	1.1
	–	–	4.0
Cu	–	–	0.5
	–	–	3.5

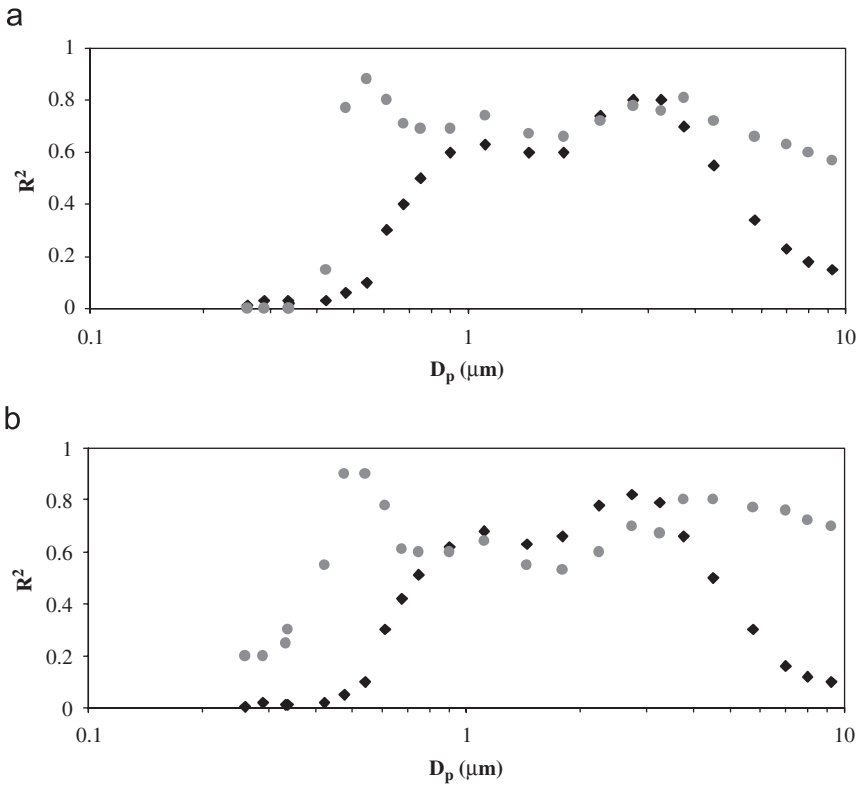

Fig. 4. Distribution of correlation coefficients between (a) Si and (b) Al, measured in Multedo and size bins, during a Saharan dust transport episode (grey circles) (7 points) and during the remaining part of the sampling period (black diamonds) (36 points).

Table 2
Apportionment of particles number in each size bin versus PM sources identified by PMF in Cornigliano, Lanterna and Multedo

Cornigliano

Dimensional class (μm)	Oil combustion (%)	Re-suspended soil (%)	Sea salt (%)	Secondary (%)	Traffic (%)	Blast furnace (%)	Zn–Pb (%)
0.30–0.40	23±4	11±4		71±3			14±3
0.40–0.50	18±7	12±5		75±5			15±6
0.50–0.65	16±7	15±5		75±7			16±5
0.65–0.80	13±5	21±5	6±3	50±4		5±3	10±4
0.80–1	11±3	30±3	14±2	25±2	5±3	11±2	4±2
1–1.6	8±3	39±3	20±2	12±2	6±3	11±2	
1.6–2	10±4	42±3	19±2	6±2	10±3	13±2	
2–3	7±4	44±3	11±2			16±2	
3–4		67±6	7±4			21±3	
4–5		71±6				17±2	
5–7.5		78±8				13±4	
7.5–10		85±9				9±9	

Lanterna

Dimensional class (μm)	Oil combustion (%)	Re-suspended soil (%)	Sea salt (%)	Secondary (%)	Traffic (%)
0.25–0.28	10±2			58±3	32±2
0.28–0.30	7±2			64±3	32±3
0.30–0.35	4±2			69±4	33±3
0.35–0.40				76±5	33±4
0.40–0.45				75±4	32±5
0.45–0.50				76±5	30±5
0.50–0.58				73±3	31±6
0.58–0.65			10±2	60±4	32±4
0.65–0.70			23±3	44±4	33±3
0.70–0.80			34±3	32±3	36±3
0.80–1			47±2	18±3	34±3
1–1.3		7±4	53±2	9±3	34±3
1.3–1.6		8±4	57±3	5±3	33±3
1.6–2		19±4	53±2		33±3
2–2.5		26±3	38±2		35±5
2.5–3		29±4	31±2		40±4
3–3.5		31±8	20±5		43±7
3.5–4		27±7	22±2		49±7
4–5		25±9	16±2		56±8
5–6.5		28±10	18±3		61±9
6.5–7.5		29±11	18±3		61±9
7.5–8.5		32±11	15±3		61±10
8.5–10		35±11	16±5		50±10

Multedo

Dimensional class (μm)	Oil combustion (%)	Re-suspended soil (%)	Sea salt (%)	Secondary (%)	Traffic (%)
0.25–0.28	5±1		5±1	74±2	15±2
0.28–0.30	6±1		6±1	78±2	15±2
0.30–0.35	4±1		8±1	75±3	18±3
0.35–0.40	3±1		10±2	69±4	23±4
0.40–0.45			12±2	58±4	32±5
0.45–0.50			14±2	45±5	39±5
0.50–0.58			19±3	34±5	44±6
0.58–0.65			26±3	23±5	46±6
0.65–0.70			31±3	19±6	44±6
0.70–0.80			34±3	19±6	41±6

Table 2 (*continued*)

Multedo					
Dimensional class (μm)	Oil combustion (%)	Re-suspended soil (%)	Sea salt (%)	Secondary (%)	Traffic (%)
0.80–1			34±3	18±5	38±6
1–1.3			34±3	18±5	37±6
1.3–1.6			36±3	19±5	38±6
1.6–2			35±3	22±5	31±6
2–2.5		11±6	26±2	24±4	29±5
2.5–3		18±6	22±2	21±4	29±4
3–3.5		24±6	25±2	13±5	31±5
3.5–4		28±6	22±2	15±5	31±5
4–5		32±7	18±2	10±5	31±5
5–6.5		40±7	12±3	10±6	29±6
6.5–7.5		43±8	9±3		31±5
7.5–8.5		44±8	8±3		29±6
8.5–10		49±9	7±3		32±7

Values compatible with zero are not shown (blank cells).

Multedo sampling site), we show the comparison between the average R^2 distribution of Al and Si averaged during the episode (which lasted 7 h) and during the remaining part of the sampling period. In the R^2 distribution data referring to the episode an increase of particles with $D_p > 4\,\mu m$ is evident; moreover, a clear and an unexpected correlation with particles sized around 0.5 μm was also found.

The multi-modal distributions, as those shown in Figs. 3 and 4, can be analyzed more quantitatively, by fitting with Gaussian curves, to obtain the value of their modes (referred to as optical diameters). In Table 1, we give the fitted modes for the elements already represented in Figs. 3 and 4 and for other tracers of PM sources (see next paragraph). During the sampling, the relative humidity ranged between 50% and 60% in all the sites. For instance, Cl, in a coastal city such as Genoa, is mainly ascribed to sea salt aerosol. According to the literature data (De Hoog et al., 2005), fresh and aged sea salt aerosols look similar in shape and size (diameter about 2 μm); a similar result was obtained by our analysis, as in all sites, Cl concentration peaked around $D_p = 1.6\,\mu m$. Sulphur is mainly produced by photochemical reactions (Seinfeld and Pandis, 1998) and therefore it is usually concentrated in fine particles: we found that the correlation coefficients distribution peaked between $D_p = 0.28\,\mu m$ (actually, the smaller resolved size) and $D_p = 0.45\,\mu m$ (see Table 1).

3.2. Source apportionment of size bins

PMF analysis of the elemental concentration time series measured by streaker samplers, resolved the number and profiles of major PM sources in each site. In this case too, we used the reduced concentration data set mentioned above.

Most of the identified sources were common to all the sites, and we called them, according to their characteristic tracers: soil (Al and Si), sea (Na, Cl, Br, coarse S), traffic (Cu, Zn, Pb), oil combustion (V, Ni) and secondary (fine S). In the industrial district of Cornigliano, PMF resolved two other sources not present elsewhere: "blast furnace", traced by high loadings of Fe and Mn, and "Zn–Pb", probably also related to the steel smelter activity. Source profiles, extracted by the hourly data set, are in agreement with those obtained in the frame of a large campaign based on daily samples (Mazzei, 2007).

The multi-linear regression performed between particles number in each size bin and PMF sources temporal trends, gives the apportionment reported in Table 2(a–c); the same results are also represented as columns plots in Fig. 5(a–c). In all sites, sea salt and re-suspended soil dust show larger contributions in the coarse fractions (soil: above $D_p = 2\,\mu m$; sea: about $D_p = 2\,\mu m$). Secondary compounds, which represent the major source of PM, and oil combustion are in the size range with $D_p < 1\,\mu m$. In Lanterna and Multedo, the traffic emissions contribution is relevant in all size bins while it

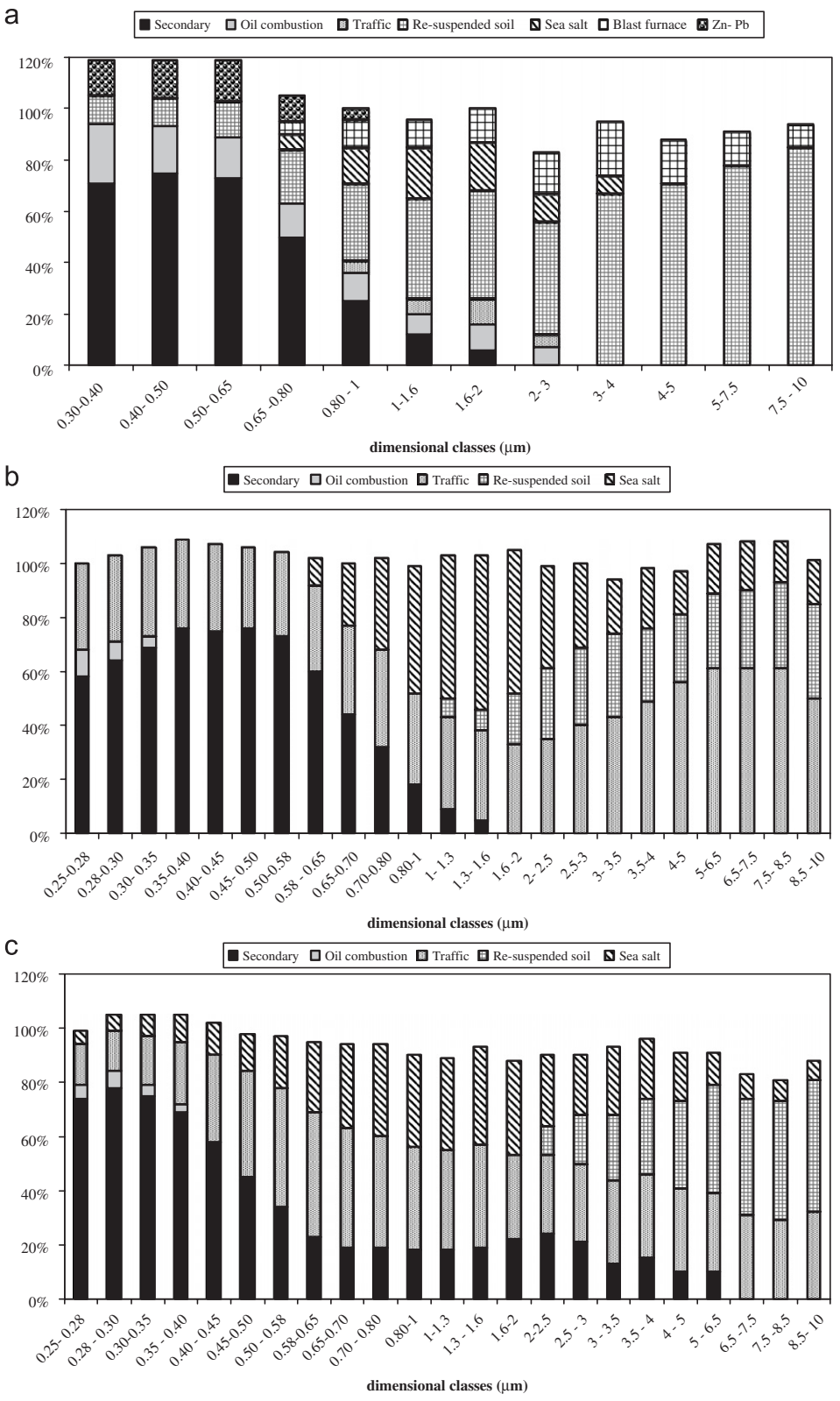

Fig. 5. Apportionment of particles number in each size bin versus the PM sources identified by PMF in (a) Cornigliano; (b) Lanterna and (c) Multedo.

represents a negligible term at the industrial site of Cornigliano. The two additional PM sources (blast furnace and "Zn–Pb") identified in Cornigliano, do not represent major contributors to local PM. The blast furnace emissions, traced by Fe, are found between $D_p = 2\,\mu m$ and $D_p = 5\,\mu m$ while the "Zn–Pb" source contributions are mainly found in particles with $D_p \leqslant 1\,\mu m$.

4. Conclusions

This study explored the effectiveness of the contemporary use of continuous PM elemental analysis, by streaker sampler and PIXE analysis, and measurement of the particle size distribution by optical methods. This approach allows us to obtain information on high-time resolution elemental size distributions and to perform the apportionment of particles number in several size classes with PM sources identified by receptor models. The field campaigns provided, in different size fractions, useful details on the impact of PM sources and on their potential adverse health effects. The methodology looks encouraging and the results suggest further developments in the direction of a faster and more powerful tool to combine size segregation and time-resolved elemental analysis. More insights could come extending the measurement to ultrafine particles (in this work 250 nm was smallest size detected by the OPC) and/or to elemental analysis with better sensitivity.

Acknowledgments

This work has been partly supported by Amministrazione Provinciale di Genova–Assessorato all' Ambiente and by I.N.F.N. We are particularly indebted with Dr. E. Daminelli for his continuous and precious collaboration. Thanks are also due to the staff of LABEC in Florence (L. Giuntini, F. Taccetti) for their assistance during PIXE irradiations. V. Ariola and A. Ripa took care of the logistic and technical problems during the sampling campaigns.

References

Annegarn, H.J., Cahill, T.A., Sellschop, J.F.P., Zucchiatti, A., 1988. Time sequence particulate sampling and nuclear analysis. Physics Scripta 37, 282–290.

Balásházy, I., Hofmann, W., Heistracher, T., 2003. Local particle deposition pattern may play a key role in the development of lung cancer. Journal of Applied Physiology 94, 1719–1725.

Binnig, J., Meyer, J., Kasper, G., 2007. Calibration of an optical particle counter to provide $PM_{2.5}$ mass for well-defined particle materials. Journal of Aerosol Science 38 (3), 325–332.

Bukowiecki, N., Hill, M., Gehrig, R., Lienemann, P., Zwicky, C.N., Hegedüs, F., Falkenberg, G., Weingartner, E., Baltensperger, U., 2005. Trace metals in ambient air: hourly size segregated mass concentrations determined by synchrotron-XRF. Environmental Science and Technology 39, 5754–5762.

Büttner, H., 1990. Measurement of the size of fine nonspherical particles with a light-scattering particle counter. Aerosol Science and Technology 12, 413–421.

Cahill, T.A., Goodart, C., Nelson, J.W., Eldred, R.A., Nasstrum, J.S., Feeney, P.J., 1987. Design and evaluation of the DRUM impactor. In: Ariman, T., Veziroglu, T.N. (Eds.), Particulate and Multiphase Processes, Vol. 2, Contamination Analysis and Control. Hemisphere Publishing Corporation, Washington, DC, USA, pp. 319–325.

Calzolai, G., Chiari, M., García Orellana, I., Lucarelli, F., Migliori, A., Nava, S., Taccetti, F., 2006. The new external beam facility for environmental studies at the Tandetron accelerator of LABEC. Nuclear Instruments and Methods in Physics Research B 249 (1–2), 928–931.

Chiari, M., Lucarelli, F., Mazzei, F., Nava, S., Paperetti, L., Prati, P., Valli, G., Vecchi, R., 2005. Airborne particulate matter characterization in an industrial district near Florence, by PIXE and PESA. X-Ray Spectrometry 34 (4), 323–329.

De Hoog, J., Osán, J., Szalóki, I., Eyckmans, K., Worobiec, A., Ro, C.-U., Van Grieken, R., 2005. Thin-window electron probe X-ray microanalysis of individual atmospheric particles above the North Sea. Atmospheric Environment 39 (18), 3231–3242.

Draxler, R.R., Rolph, G.D., 2003. HYSPLIT (Hybrid Single-Particle Lagrangian Integrated Trajectory) model access via NOAA ARL READY website ⟨http://www.arl.noaa.gov/ready/hysplit4.html⟩. NOAA Air Resources Laboratory, Silver Spring, MD.

Fissan, H., Helsper, C., Kasper, W., 1984. Calibration of optical particle counters with respect to particle size. Particle Characterization 1, 108–111.

Gordon, G.E., 1988. Receptor models. Environmental Science and Technology 22, 1132–1142.

Hand, J.L., Kreidenweis, S.M., 2002. A new method for retrieving particle refractive index and effective density from aerosol size distribution data. Aerosol Science and Technology 36, 1012–1026.

HEI Review Committee (HEI), 2002. Understanding the Health Effects of Components of the Particulate Matter: Progress and Next Steps. Health Effect Institute, Boston.

Hillamo, R., Kauppinen, E.I., 1991. On the performance of the Berner low pressure impactor. Aerosol Science and Technology 14, 33–47.

Knutson, E.O., Whitby, K.T., 1975. Aerosol classification by electric mobility: apparatus, theory and applications. Journal of Aerosol Science 6, 443–451.

Lee, E., Chan, C.K., Paatero, P., 1999. Application of positive matrix factorization in source apportionment of particulate pollutants in Hong Kong. Atmospheric Environment 33, 3201–3212.

Maenhaut, W., Hillamo, R., Mäkelä, T., Jaffrezo, J.L., Bergin, M.H., Davidson, C.I., 1996. A new cascade impactor for aerosol sampling with subsequent PIXE analysis. Nuclear Instruments and Methods B 109/110, 482–487.

Marple, V.A., Rubow, K.L., Behm, S.M., 1991. A Microorifice Uniform Deposit Impactor (MOUDI): description, calibration, and use. Aerosol Science and Technology 14, 434–446.

Maxwell, J.A., Teesdale, W.J., Campbell, J.L., 1995. The Guelph PIXE package II. Nuclear Instruments and Methods in Physics Research B 95, 407–421.

Mazzei, F., 2007. Characterization of atmospheric aerosol sources: an open field experiment. PhD Thesis, University of Genova (IT).

Paatero, P., Tapper, U., 1994. Positive matrix factorization: a non-negative factor model with optimal utilization of error estimates of data values. Environmetrics 5, 111–126.

Paatero, P., Hopke, P.K., Song, X., Ramadan, Z., 2002. Understanding and controlling rotations in factor analytical models. Chemometrics and Intelligent Laboratory Systems 60, 253–264.

Polissar, A.V., Hopke, P.K., Paatero, P., Malm, W.C., Sisler, J.F., 1998. Atmospheric aerosol over Alaska 2. Elemental composition and sources. Journal of Geophysical Research 103, 19045–19057.

Pope III, C.A., Burnett, R.T., Thun, M.J., Calle, E.E., Krewski, D., Ito, K., Thurston, G.D., 2002. Lung cancer, cardiopulmonary mortality, and long-term exposure to fine particulate air pollution. Journal of American Medical Association 287, 1132–1141.

Prati, P., Zucchiatti, A., Lucarelli, F., Mandò, P.A., 2000. Source apportionment near a steel plant in Genoa by continuous aerosol sampling and PIXE analysis. Atmospheric Environment 34 (19), 3149–3157.

Putaud, J.P., Van Dingenen, R., Dell'Acqua, A., Raes, F., Matta, E., Decesari, S., Facchini, M.C., Fuzzi, S., 2004. Size-segregated aerosol mass closure and chemical composition in Monte Cimone (I) during MINATROC. Atmospheric Chemistry and Physics 4, 889–902.

Salma, I., Ocskay, R., Raes, N., Maenhaut, W., 2005. Fine structure of mass size distributions in an urban environment. Atmospheric Environment 39, 5363–5374.

Seinfeld, J.H., Pandis, S.N., 1998. Atmospheric Chemistry and Physics. Wiley, New York.

Wichmann, H.E., Peters, A., 2000. Epidemiological Evidence of the Effects of Ultra Fine Particle Exposure. Philosophical transactions of the Royal Society, London. University Press, Cambridge, pp. 2751–2770.

Winklmayr, W., Reischl, G.P., Lindner, A.O., Berner, A., 1991. A new electromobility spectrometer for the measurement of aerosol size distributions in the size range from 1 to 1000 nm. Journal of Aerosol Science 22, 289–296.